Trees (2002) 16:457–464
DOI 10.1007/s00468-002-0186-2

ORIGINAL ARTICLE

Masato Yoshida · Haruki Ohta · Hiroyuki Yamamoto
Takashi Okuyama

Tensile growth stress and lignin distribution in the cell walls of yellow poplar, *Liriodendron tulipifera* Linn.

Received: 9 July 2001 / Accepted: 8 April 2002 / Published online: 25 May 2002

Abstract Five specimens that contained a continuous gradient of wood, from normal to tension wood regions, were collected from an inclined yellow poplar (*Liriodendron tulipifera*), and the released strain of tensile growth stress was quantified. Ultraviolet (UV) microspectrophotometry was used to examine the relationship between lignin distribution in the cell wall and the intensity of tensile growth stress. The UV absorption of the secondary wall and the cell corner middle lamella decreased with increasing tensile released strain (i.e., tensile growth stress). The UV absorption in the compound middle lamella region remained virtually constant, irrespective of the tensile released strain. The absorption maximum (λ_{max}) remained virtually constant in the secondary wall, the cell corner middle lamella, and the compound middle lamella region at 273–274, 277–278, and 275–278 nm respectively, irrespective of the tensile released strain. The ratios of the UV absorbance at 280 to 260 nm and 280 to 273 nm of the secondary wall decreased with increasing tensile released strain. The ratios in the cell corner and compound middle lamella region remained constant, irrespective of the tensile released strain. The lignin content of the secondary wall decreased, while the syringyl/guaiacyl ratio increased with increasing tensile released strain. Gelatinous fibers were not observed in the tension wood regions, but the secondary wall became gelatinous-layer-like, i.e., the lignin content and microfibrillar angle decreased and the cellulose content increased. A definite gelatinous layer seems to be important for generating greater tensile growth stress. It is concluded that a decrease in lignin and an increase in cellulose microfibrils parallel to the fiber axis in the secondary wall are necessary to produce large tensile growth stress.

M. Yoshida (✉) · H. Ohta · H. Yamamoto · T. Okuyama
Laboratory of Bio-Material Physics,
Graduate School of Bioagricultural Sciences, Nagoya University,
Nagoya 464–8601, Japan
e-mail: yoshida@agr.nagoya-u.ac.jp
Fax: +81-52-789-4150

Keywords Gelatinous layer · Lignin distribution · UV microspectrophotometry · Tensile growth stress · Tension wood

Introduction

Tension wood is the reaction wood that typically forms in the upper sides of branches and leaning trunks of dicotyledonous trees. It is characterized anatomically by a lack of cell wall lignification, and often by the presence of an internal gelatinous (G-) layer in the fibers (IAWA 1964; Wardrop 1965; Ford-Robertson 1971; Fisher 1985). Based on the patterns of occurrence of the gelatinous layer, tension wood fibers have been classified into the following: S_1+S_2+S_3+G, S_1+S_2+G, and S_1+G (Dadswell and Wardrop 1955). The main feature of the gelatinous layer is that it is composed entirely or almost entirely of cellulose, with microfibrils oriented parallel or nearly parallel to the longitudinal axis, with a high degree of crystallinity (Côté and Day 1965; Norberg and Meier 1966). Some angiosperm species lack gelatinous fibers in tension wood (Onaka 1949; Okuyama et al. 1990, 1994; Yoshizawa et al. 2000). In some *Magnolia* species that do not form a gelatinous layer, the microfibrillar angle (MFA) in the innermost layer of fiber walls is small and the amount of lignin decreases in the tension wood region (Yoshizawa et al. 2000). Members of the genus *Magnolia* are considered primitive angiosperms that lack gelatinous fibers in tension wood.

In tension wood, longitudinal tensile growth stress increases in order to restore the trunk to its original vertical position (Nicholson 1973; Baillères et al. 1995; Mattheck and Kubler 1995; Wilson and Gartner 1996; Yoshida et al. 1999). Bamber (1987) attributed the origin of tensile growth stress to the tensile force induced in cellulose microfibril bundles. Experimental results and model analyses support his idea. Increasing tensile growth stress is correlated with decreasing MFA and Klason lignin content, and increasing alpha-cellulose

content and cellulose crystallinity (Okuyama et al. 1990). These correlations clarified the contribution of cellulose microfibrils to tensile growth stress generation (Yamamoto et al. 1992), and subsequent numerical analyses showed that greater tensile growth stress is generated in the gelatinous layer (Yamamoto et al. 1993a).

Large longitudinal tensile growth stresses can even be generated in the tension wood of trees that do not produce gelatinous fibers (Okuyama et al. 1990; Yoshida et al. 2000a). In these tree species, tensile growth stress increases with increasing alpha-cellulose content and cellulose crystallinity, and decreasing MFA and Klason lignin content, similar to that found in gelatinous fibers (Sugiyama et al. 1993; Okuyama et al. 1994; Yamamoto 1998).

Cellular ultraviolet (UV) microspectrophotometry has shown that compressive growth stress is associated with a higher lignin content in the secondary wall in compression wood of *Cryptomeria japonica* (Okuyama et al. 1998). In the tension wood of *Robinia pseudoacacia*, the gelatinous layer begins to differentiate and its lignin content begins to decrease with increasing tensile growth stress (Yoshida et al. 2002). In the tension wood of tree species that do not form gelatinous fibers, the lignin content of the secondary wall probably decreases with increasing tensile growth stress. The gelatinous layer may be specialized for generating larger tensile growth stress.

To test this hypothesis and to examine any relationship to tensile growth stress, this study used UV microspectrophotometry to investigate lignin distribution in the cell wall in tension wood of *Liriodendron tulipifera*, which does not form gelatinous fibers.

Materials and methods

Three inclined 51-year-old yellow poplar trees (*Liriodendron tulipifera* Linn.), on average 14 m tall and 30 cm in diameter at breast height, growing in West Virginia, were studied. This species lacks gelatinous fibers on the upper side of inclined stems (Onaka 1949; Sugiyama et al. 1993).

Measuring growth stress and wood properties

Eight to 14 measuring points were established around the circumference of the trunk, where the trunk was bent severely. Measurements were made in each tree on two circumferences, so in total 6 circumferences and 67 points were measured. A strain-gauge method was used on the standing tree (Yoshida and Okuyama 2002). The bark, phloem, and thin cambial zone at each measuring point were carefully removed with a knife without scratching the outer surface of the secondary xylem. At each point, two 8-mm-long strain gauges were glued to the outer surface of the secondary xylem, one longitudinally and one tangentially, and connected to a strain meter. After initial measurements had been made in the standing position, grooves were cut with a thin saw to the depth of the current growth layer (about 1 cm), 5 mm from each end of the strain gauge, to release the growth stress. The larger the tensile strain released, the higher the tensile growth stress (Archer 1986) and the greater the intensity of tension wood formation.

After measuring the released strain, block specimens were obtained of the wood directly above each measuring point to determine elastic modulus, density, MFA, and cellulose crystallinity. The elastic modulus was determined by a tensile test using small (10×20×1-mm) test specimens of green wood. The elastic moduli in the longitudinal and tangential directions and Poisson's ratios were measured to convert the released strains to growth stresses. Longitudinal and tangential growth stresses (σ_L, σ_T) were calculated as follows (Sasaki et al. 1978):

$$\begin{aligned} \sigma_L &= E_L \frac{\varepsilon_L + \nu_{TL}\varepsilon_T}{1-\nu_{TL}\nu_{LT}} \\ \sigma_T &= E_T \frac{\varepsilon_T + \nu_{TL}\varepsilon_T}{1-\nu_{TL}\nu_{LT}} \end{aligned} \quad (1)$$

where E_L and E_T are the elastic moduli in the longitudinal and tangential directions, respectively, ε_L and ε_T are the released strains in the longitudinal and tangential directions, and ν_{TL} and ν_{LT} are Poisson's ratio.

The density of air-dried specimens was measured using a gravimetric mercury method. MFA was determined by an improved version of Cave's method (Yamamoto et al. 1993b). The cellulose crystallinity was measured by X-ray diffraction. Other wood block specimens were obtained from directly below each measuring position to determine chemical components; Klason-lignin and alpha-cellulose content were determined using methods in general use (Dence 1992; Sugiyama et al. 1993). The radius vector defined as the distance from the pith to the xylem surface was measured at every point at which the released strain was measured.

UV microspectrophotometry

Five specimens, with growth stress ranging from normal wood to tension wood, were selected for UV spectral analysis. Small blocks of xylem tissue containing the current growth layer were obtained from the measuring points and fixed with 3% glutaraldehyde. Vertical sections with a thickness of 200 µm were sliced from the blocks using a sliding microtome. After dehydration through a graded ethanol series, the sections were piled together and embedded in epoxy resin. Cross sections with a thickness of 1 µm were cut with a diamond knife, mounted on quartz microscope slides, immersed under a drop of non-UV-absorbing glycerin, and covered with a quartz cover slip. The thickness of each thin section was measured with an accuracy of 0.01 µm with a universal surface shape profiler (Kosaka, SE-3E), to select sections with uniform thickness and to correct the UV absorption spectra (Okuyama et al. 1998). The thin sections were observed at wavelengths of 270–280 nm under a microspectrophotometer (Zeiss MPM800). The UV absorption spectra of the cell corner middle lamella, compound middle lamella, and secondary wall were obtained for wavelengths of 250–300 nm using the smallest measuring spot available with the microspectrophotometer (0.5 µm diameter). Since the spot diameter was larger than the width of the middle lamella, measurements of the latter were affected by the secondary wall. To reduce this error, the spot measured was centered on the middle lamella and any peculiar spectra were omitted. This region was named the "compound middle lamella region". Measurements were taken from at least 15 different positions and averaged to determine the UV absorption spectra. The microspectrophotometer settings were: objective lens magnification: ×100; program: Lambdascan; bandwidth: 1 nm; scan step: 1 nm; and number of scans: 45. For more detailed information see Scott and Goring (1970), Okuyama et al. (1998), and Gindl and Okuyama (1999).

Results

Released strain of growth stress and wood properties

The strain gauge method used in this study reveals tensile growth stress as a negative released-strain (tensile released strain) value. Eccentric growth was found in all six disks measured on the upper side of the leaning

Table 1 Growth stress and other selected properties of the specimens used for the microspectrophotometry. (*MFA* microfibrillar angle)

Specimen label	Released strain (%)	Young's modulus (GPa)	Density in air-dried condition (g/cm^3)	Growth stress in L-direction (MPa)	Cellulose content (%)	Cellulose crystallinity (%)	Lignin content (%)	MFA (degrees)	Radius vector (cm)
a	0.0082	7.56	0.344	–0.56	40.65	41.94	12.65	16.25	11.0
b	–0.0409	10.72	0.454	4.53	45.04	38.88	14.37	8.24	13.0
c	–0.0757	10.48	0.344	7.94	47.94	41.94	12.90	7.36	9.8
d	–0.1201	16.01	0.447	19.33	50.35	43.51	10.21	7.92	13.2
e	–0.1499	10.21	0.403	15.39	48.64	43.46	11.09	8.13	18.0

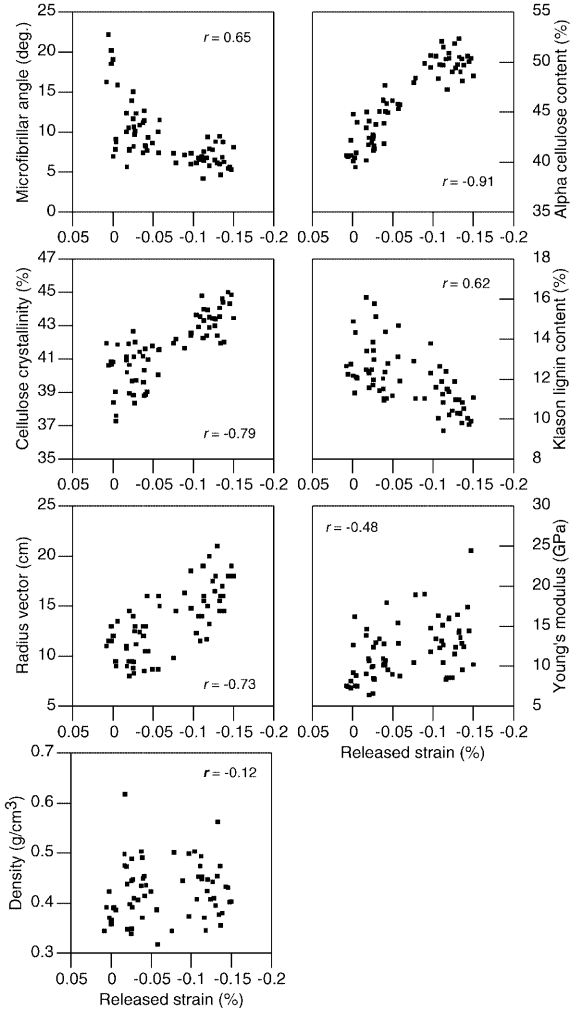

Fig. 1 Released strain of growth stress and wood properties. Negative released strain indicates the tensile released strain measured when releasing tensile growth stress

trunk, where the largest tensile released strains were measured. The smallest tensile released strains were measured on the opposite, lower side. Figure 1 shows the relationships between the released strain and various properties for all 67 measuring points. The tensile released strain increased with decreasing MFA and Klason-lignin content, and increasing alpha-cellulose content, cellulose crystallinity, radius vector, and longitudinal Young's modulus (in all cases $P<0.001$). There was no significant correlation between the released strain and density ($P=0.34$). Five specimens, ranging from normal wood to tension wood, were selected for UV spectral analysis and observation. The released strains and properties of the specimens selected for microspectrophotometry are tabulated in Table 1.

UV micrograph

Figure 2 shows micrographs and absorption profiles across the cell walls of fibers at a wavelength of 278 nm. Results similar to the following were obtained for wavelengths of 270–280 nm. In normal wood specimens with 0.0082% released strain (Fig. 2a), the UV absorbance was high in the cell corner middle lamella and compound middle lamella, and low in the secondary wall. As the tensile released strain increased, the UV absorbance of the secondary wall decreased (Fig. 2b–d), and was lowest in the specimen with the largest tensile released strain (–0.1499%, Fig. 2e). In these fibers, the absorption profiles indicated that the inner layer of the secondary wall had a higher absorbance than the outer layer. The absorption profiles change abruptly from Fig. 2d to e. The thickness of the fiber cell wall remained constant irrespective of the released strain, whereas fiber diameter decreased with increasing tensile released strain ($r=0.6$, $P<0.001$).

UV absorption spectra

The average UV absorption spectra for the cell corner middle lamella, compound middle lamella region, and secondary wall are shown in Fig. 3. In the cell corner middle lamella, the UV absorption decreased with increasing tensile released strain ($r=0.34$, $P=0.001$), and the absorption maximum (λ_{max}) was 277–278 nm. In the compound middle lamella region, λ_{max} was 275–278 nm, and the UV absorption remained constant, irrespective of the tensile released strain ($r=–0.18$, $P=0.095$). In the secondary wall of normal wood (Fig. 3a), or wood with a small tensile released strain value (Fig. 3b, c), λ_{max} was 273–274 nm. In the secondary wall of tension wood with a large tensile released strain value (Fig. 3d, e), λ_{max} was unclear. The UV absorption of the secondary wall de-

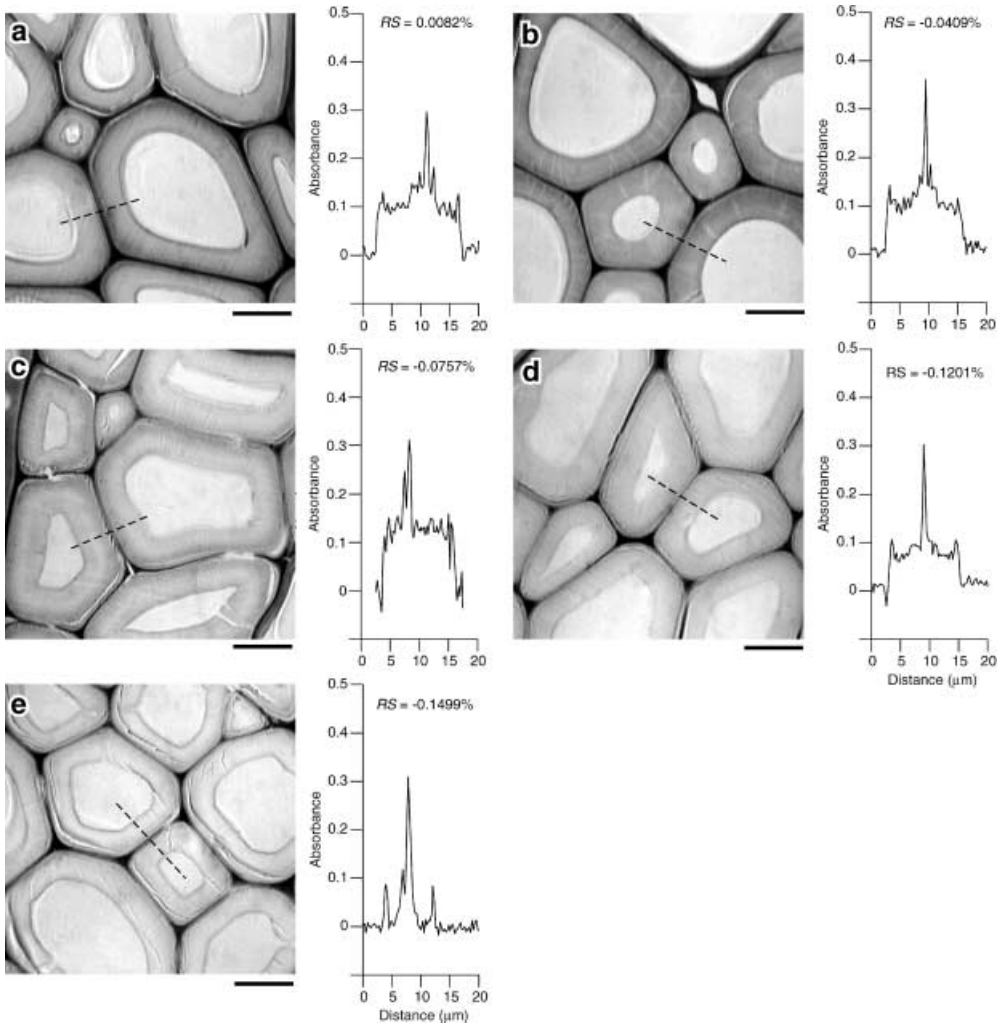

Fig. 2 Ultraviolet (UV) photomicrographs of cross-sectional and absorption profiles across the cell walls of fibers at a wavelength of 278 nm in samples graded according to the released strain (*RS*) of growth stress, from normal wood (*a*) to tension wood (*e*). The *dotted lines* indicate the positions of absorption profiles. *Bar*=10 μm

creased with increasing tensile released strain (r=0.37, P=0.002).

Discussion

The released strain of growth stress is used to obtain a continuous, quantitative classification of wood samples, because there is a high correlation between the released strain and the intensity of reaction wood (Yamamoto et al. 1991; Sugiyama et al. 1993; Okuyama et al. 1994; Muneri et al. 1999). The released strain is therefore effective for estimating the intensity of reaction wood, especially when the reaction wood is not characterized anatomically (Baillères et al. 1995, 1997; Plomion et al. 2000; Yoshida et al. 2000b). The five specimens measured in this study using microspectrophotometry ranged from normal wood (Fig. 2a) to intense tension wood (Fig. 2e).

The tensile growth stress was found to increase with decreasing MFA and Klason lignin content, as well as with increasing alpha-cellulose content, cellulose crystallinity, and radius vector (Fig. 1). These results are similar to those obtained in tree species that form gelatinous fibers (Okuyama et al. 1990).

Decreasing UV absorption reflects decreasing lignin content (Fergus and Goring 1970a, 1970b; Nakashima et al. 1997; Donaldson et al. 1999; Gindl et al. 2000; Kleist and Bauch 2001; Sander and Koch 2001; Suzuki and Itoh 2001). With increasing tensile released strain, the UV absorption, and therefore the lignin content, of the secondary wall decreased (Table 2).

Jutte (1956) found a lignified layer in the gelatinous layer of *Ocotea rubra* and showed that an unlignified cell wall might be the first phase of tension wood differentiation. UV micrographs of some hardwood species show that lignin often penetrates the gelatinous layer, and that cells in transition regions between normal and tension wood are more likely to have lignin deposited in the gelatinous layer than are cells in the center of an area of tension wood (Scurfield and Wardrop 1963). Araki et al. (1982) also compared the cell wall structure of transition fibers in normal and tension wood in *Robinia pseudoacacia* L. and *Populus euramericana* Guinier, and found that concentric rings stained with $KMnO_4$ did not exist in definitive gelatinous layers, but were present in transitional gelatinous layers. A comparison of a progression of fibers, from normal wood to those of the indefinite gelatinous layer, in *R. pseudoacacia*, showed

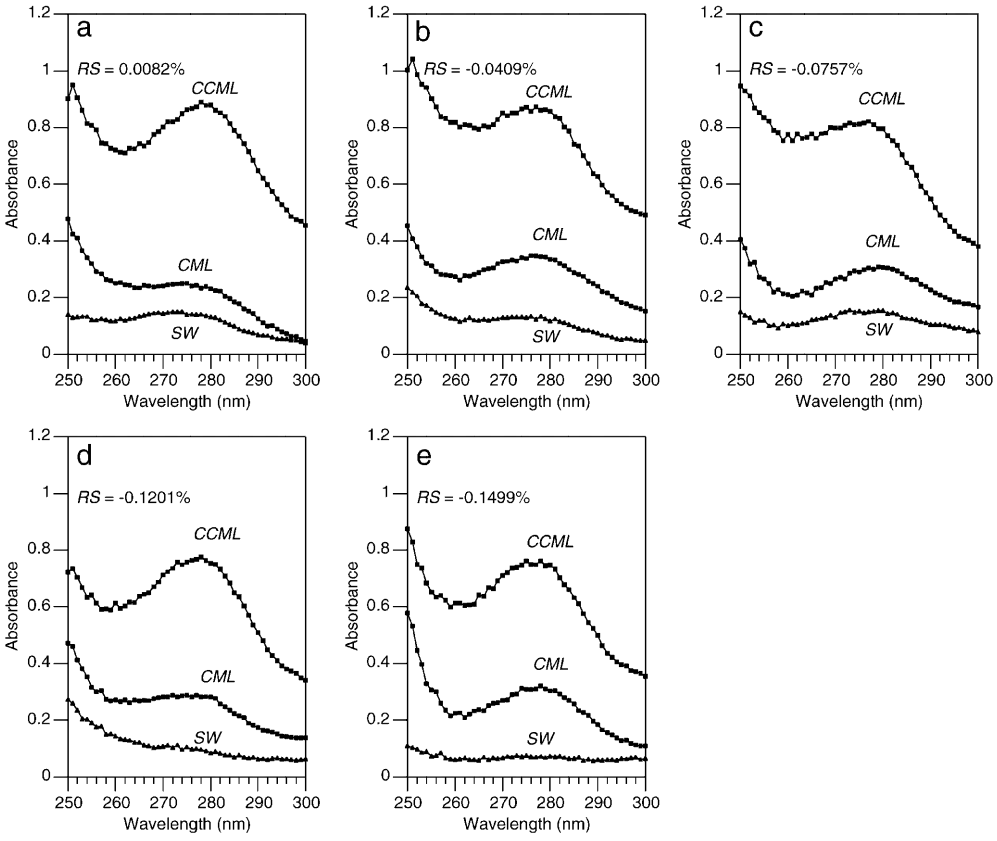

Fig. 3 UV absorption spectra of the cell corner middle lamella (*CCML*), the compound middle lamella region (*CML*), and the secondary wall (*SW*) of fibers in samples graded according to the released strain (*RS*) of growth stress, from normal wood (*a*) to tension wood (*e*)

Table 2 Absorbance at wavelength 278 nm and λ_{max} in various regions of cell walls of fibers in samples graded according to the released strain of growth stress. (*CCML* cell corner middle lamella, *CML* compound middle lamella region, *SW* secondary wall. The standard deviation is given in parentheses)

Specimen label	Released strain (%)	Absorbance Region of cell wall			λ_{max} (nm) Region of cell wall		
		CCML	CML	SW	CCML	CML	SW
a	0.0082	0.88 (0.17)	0.23 (0.07)	0.13 (0.03)	278 (1.1)	275 (1.6)	273 (1.9)
b	–0.0409	0.86 (0.18)	0.34 (0.07)	0.12 (0.02)	278 (1.7)	276 (2.0)	273 (1.9)
c	–0.0757	0.82 (0.11)	0.28 (0.11)	0.14 (0.06)	278 (1.3)	278 (2.8)	274 (2.2)
d	–0.1201	0.77 (0.13)	0.29 (0.10)	0.09 (0.03)	278 (1.1)	275 (2.7)	–
e	–0.1499	0.72 (0.20)	0.31 (0.10)	0.06 (0.02)	277 (0.9)	276 (2.1)	–

that the UV absorbance of the secondary wall decreased as the tensile released strain increased (Yoshida et al. 2002). On the basis of the examples quoted above and the results of this study, in the transition from normal wood to tension wood of increasing intensity, the degree of lignification of the secondary wall gradually decreases (Fig. 2a–d), causing the unlignified layers to develop into gelatinous layers. In the last phase of tension wood differentiation, the lignin content seems to change abruptly (Fig. 2d, e). The tensile growth stress measured in *Liriodendron tulipifera*, which does not form gelatinous fibers, is smaller than that measured in *R. pseudoacacia*, which does form gelatinous fibers (Yoshida et al. 2002). Specialization of the cell wall into a gelatinous layer seems to occur in order to generate greater tensile growth stress.

The absence of gelatinous fibers in *L. tulipifera* seems to be related to the decreasing lignin content in the cell corner middle lamella with increasing tensile growth stress. The UV absorption of the secondary wall and the cell corner middle lamella decreased with increasing tensile released strain. The UV absorption of the compound middle lamella region remained virtually constant, irrespective of the tensile released strain (Table 2).

The decreased lignin content and MFA of the secondary wall, which are characteristics of gelatinous layers, are needed, in order to generate a large tensile growth stress. A lower lignin content in the cell corner middle lamella, however, seems to be disadvantageous for the generation of a large tensile growth stress, for the following reason. Tensile growth stress is produced as fibers tend to shrink (Bamber 1987; Mattheck and Kubler 1995;

Table 3 Ratio of Absorbance at wavelengths 280 nm to 260 nm and to 273 nm in various regions of fiber cell walls in samples graded according to the released strain of growth stress. (*CCML* cell corner middle lamella, *CML* compound middle lamella region, *SW* secondary wall. The standard deviation is given in parentheses)

Specimen label	Released strain (%)	CCML		CML		SW	
		280/260	280/273	280/260	280/273	280/260	280/273
a	0.0082	1.27 (0.08)	1.04 (0.03)	1.13 (0.24)	0.95 (0.06)	1.14 (0.18)	0.90 (0.07)
b	–0.0409	1.20 (0.11)	1.03 (0.03)	1.26 (0.25)	0.99 (0.04)	1.07 (0.12)	0.93 (0.09)
c	–0.0757	1.16 (0.31)	0.96 (0.23)	1.39 (0.47)	1.05 (0.05)	1.28 (0.36)	0.93 (0.13)
d	–0.1201	1.26 (0.15)	1.01 (0.01)	1.14 (0.38)	0.96 (0.07)	0.65 (0.20)	0.78 (0.25)
e	–0.1499	1.24 (0.12)	1.02 (0.04)	1.12 (0.13)	1.00 (0.05)	0.92 (0.27)	0.86 (0.14)

Hejnowicz 1997). The lignin in the cell corner and compound middle lamella cements fibers together strongly, ensuring the transmission of large tensile growth stresses through the wood. In the tension wood of *R. pseudoacacia*, which forms gelatinous fibers, the amounts of lignin in the cell corner and compound middle lamella do not decrease (Yoshida et al. 2002), whereas in the tension wood of *L. tulipifera*, which does not form gelatinous fibers, the amount of lignin in the cell corner middle lamella does decrease. Consequently, large tensile growth stress does not seem to be efficiently transmitted through the wood.

The UV absorption properties of hardwood lignins in the 280-nm region depend markedly on the ratio of syringylpropane (S) to guaiacylpropane (G) units, but they are not effective in quantifying hardwood lignin. Accurate measurement of the S/G ratio by UV spectroscopy is difficult, because the λ_{max} values of S and G units are similar: 270 and 280 nm, respectively. Moreover, S and G lignins have different UV absorptivity. However, changes in the S/G ratio can be estimated from the UV absorption spectra. The S/G ratio increases as λ_{max} in the spectrum decreases from 280 nm (Fergus and Goring 1970a; Yoshinaga et al. 1992). Decreases in the ratios of the UV absorbance at 280 nm to that at 260 nm (A_{280}/A_{260}) and at 280 nm to 273 nm (A_{280}/A_{273}) correspond to an increasing S/G ratio (Fergus and Goring 1970a; Musha and Goring 1975; Fujii et al. 1987).

In the secondary wall λ_{max} remained virtually constant, the cell corner middle lamella, and the compound middle lamella region, irrespective of the tensile released strain (Table 2). A_{280}/A_{273} and A_{280}/A_{260} in the cell corner middle lamella and the compound middle lamella region remained constant, irrespective of the tensile released strain. In the secondary wall, A_{280}/A_{260} decreased with increasing tensile released strain (r=0.39, P<0.001) and A_{280}/A_{273} tended to decrease (r=0.22, P=0.063) (Table 3). These results suggest that the S/G ratio in the secondary wall increases with the tensile released strain. In *Eucalyptus* (Baillères et al. 1995) and *R. pseudoacacia* (Yoshida et al. 2002), the lignin in the secondary wall becomes S lignin-rich with increasing intensity of tension wood. Yoshizawa et al. (2000) showed that G lignin decreased in the cell wall of tension wood fibers in *Magnolia obovata* and *M. kobus*. The results of this study on *L. tulipifera* are consistent with these reports.

In some poplar species, there are no peaks in the UV absorption spectra of the fiber walls because the absorbance characteristics of the *p*-hydroxy benzoic acid groups distort the syringyl and guaiacyl spectra. If some *p*-hydroxy benzoic acid residues are associated with syringyl residues, the peak shifts to a lower wavelength or disappears altogether (Musha and Goring 1975). However, since the UV absorption spectra of *L. tulipifera* have a peak (Fig. 3), they are not affected by the *p*-hydroxy benzoic acid residues. Microautoradiograms of differentiating xylem tissues indicate that three kinds of monolignol units are incorporated into different stages of cell wall formation, in the order: *p*-hydroxyphenyl, guaiacyl, and syringyl units (Terashima and Fukushima 1989). *p*-Hydroxyphenyl units are incorporated only in the earliest stage, mainly into the cell corner and middle lamella, and are not found in the secondary wall lignin in angiosperm fibers (Terashima et al. 1993; Terashima 2000). Therefore, the *p*-hydroxyphenyl units did not affect the change of the UV spectra of the secondary wall in this study.

The transverse diameters of tension wood fibers are 20% smaller than those of normal wood fibers in *M. obovata*, *Paulownia tomentosa*, and *Firmiana platanifolia*, which do not form gelatinous fibers (Li and Fujita 1997). The tension wood fibers in *L. tulipifera* were also smaller.

Conclusions

Lignin distribution in the cell wall and its relation to tensile growth stress were investigated in *L. tulipifera*, which does not form gelatinous fibers in tension wood regions. The lignin content and MFA in the secondary wall decreased and the alpha-cellulose content increased with increasing tensile released strain. A definite gelatinous layer seems to differentiate in order to generate greater tensile growth stress. A series of investigations of growth stress generation with UV microspectrophotometry (Okuyama et al. 1998; Yoshida et al. 2002), including this study, lead to the following conclusion. Growth stress is generated mainly at the secondary wall of wood fibers. Increasing cellulose content and decreasing lignin content and MFA in the secondary wall increase tensile growth stress, while decreasing cellulose and increasing

lignin and MFA increase compressive growth stress. The wide variation in growth stress, from the large tensile growth stresses induced in tension wood through normal growth stress induced in normal wood to the large compressive growth stresses induced in compression wood, results from differences in the lignin and cellulose contents, and the MFA of the secondary wall. When growth stress functions to return the axis of a leaning tree to the perpendicular, the change from normal wood to reaction wood is continuous.

References

Araki N, Fujita M, Saiki H, Harada H (1982) Transition of the fiber wall structure from normal wood to tension wood in *Robinia pseudoacacia* L. and *Populus euramericana* Guinier. Mokuzai Gakkaishi 28:267–273

Archer RR (1986) Growth stresses and strains in trees. Springer, Berlin Heidelberg New York

Baillères H, Chanson B, Fournier M, Tollier MT, Monties B (1995) Wood structure, chemical composition and growth strains in *Eucalyptus* clones (in French). Ann Sci For 51:157–172

Baillères H, Castan M, Monties B, Pollet B, Lapierre C (1997) Lignin structure in *Buxus sempervirens* reaction wood. Phytochemistry 44:35–39

Bamber RK (1987) The origin of growth stresses. IAWA Bull 8:80–84

Côté WA Jr, Day AC (1965) Anatomy and ultrastructure of reaction wood. In: Côté WA Jr (ed) Cellular ultrastructure of woody plants. Syracuse University Press, Syracuse, pp 391–418

Dadswell HE, Wardrop AB (1955) The structure and properties of tension wood. Holzforschung 9:97–104

Dence CW (1992) The determination of lignin. In: Lin SY, Dence CW (eds) Methods in lignin chemistry. Springer, Berlin Heidelberg New York, pp 33–61

Donaldson LA, Singh AP, Yoshinaga A, Takabe K (1999) Lignin distribution in mild compression wood *Pinus radiata*. Can J Bot 77:41–50

Fergus BJ, Goring DAI (1970a) The location of guaiacyl and syringyl lignins in birch xylem tissue. Holzforschung 24:113–117

Fergus BJ, Goring DAI (1970b) The distribution of lignin in birch wood as determined by ultraviolet microscopy. Holzforschung 24:118–124

Fisher JB (1985) Induction of reaction wood in *Terminalia* (Combretaceae): roles of gravity and stress. Ann Bot 55:237–248

Ford-Robertson FC (1971) Terminology of forest science, technology, practice, and products. Society of American Foresters, Washington, D.C.

Fujii T, Shimizu K, Yamaguchi A (1987) Enzymatic saccharification on ultrathin sections and ultraviolet spectra of Japanese hardwoods and softwoods. Mokuzai Gakkaishi 33:400–407

Gindl W, Okuyama T (1999) Increase of error in lignin measurement using ultraviolet microscopy due to multiple scanning. J Wood Sci 45:179–180

Gindl W, Grabner M, Wimmer R (2000) The influence of temperature on latewood lignin content in tree line Norway spruce compared with maximum density and ring width. Trees 14:409–414

Hejnowicz Z (1997) Graviresponses in herbs and trees: a major role for the redistribution of tissue and growth stresses. Planta 203:S136-S146

IAWA Committee (1964) Multilingual glossary of terms used in wood anatomy. Konkordia, Winterthur

Jutte SM (1956) Tension wood in wane (*Ocotea rubra* Mez). Holzforschung 10:33–35

Kleist G, Bauch J (2001) Cellular UV microspectrophotometric investigation of sapelli heartwood (*Entandrophragma cylindricum* Sprangue) from natural provenances in Africa. Holzforschung 55:117–122

Li Y, Fujita M (1997) Abstracts of the 47th annual meeting of the Japan wood research society (in Japanese). Japan Wood Research Society, Tokyo

Mattheck C, Kubler H (1995) Wood: the internal optimization of trees. Springer, Berlin Heidelberg New York

Muneri A, Leggate W, Palmer G (1999) Relationships between surface growth strain and some trees. Wood and sawn timber characteristics of *Eucalyptus cloeziana*. S Afr For J 186:41–49

Musha Y, Goring DAI (1975) Distribution of syringyl and guaiacyl moieties in hardwoods as indicated by ultraviolet microscopy. Wood Sci Technol 9:45–58

Nakashima J, Mizuno T, Takabe K, Fujita M, Saiki H (1997) Direct visualization of lignifying secondary wall thickenings in *Zinnia elegans* cells in culture. Plant Cell Physiol 38:818–827

Nicholson JE (1973) Growth stress differences in *Eucalyptus*. For Sci 19:169–174

Norberg PH, Meier H (1966) Physical and chemical properties of the gelatinous layer in tension wood fibers of aspen (*Populus tremula* L.). Holzforschung 20:174–178

Okuyama T, Yamamoto H, Iguchi M, Yoshida M (1990) Generation process of growth stresses in cell walls. II. Growth stresses in tension wood. Mokuzai Gakkaishi 36:797–803

Okuyama T, Yamamoto H, Yoshida M, Hattori Y, Archer RR (1994) Growth stresses in tension wood: role of microfibrils and lignification. Ann Sci For 51:291–300

Okuyama T, Takeda H, Yamamoto H, Yoshida M (1998) Relation between growth stress and lignin concentration in the cell wall: ultraviolet microscopic spectral analysis. J Wood Sci 44:83–89

Onaka F (1949) Studies on compression- and tension-wood (in Japanese). Wood Res 1:1–88

Plomion C, Pionneau C, Brach J, Costa P, Baillères H (2000) Compression wood-responsive proteins in developing xylem of maritime pine (*Pinus pinaster* Ait.). Plant Physiol 123:959–969

Sander C, Koch G (2001) Effects of acetylation and hydrothermal treatment on lignin as revealed by cellular UV-spectroscopy in Norway spruce (*Picea abies* [L.] Karst.). Holzforschung 55:193–198

Sasaki Y, Okuyama T, Kikata Y (1978) The evolution process of the growth stress in the tree: the surface stresses on the tree. Mokuzai Gakkaishi 24:149–157

Scott JAN, Goring DAI (1970) Photolysis of wood microsections in the ultraviolet microscope. Wood Sci Technol 4:237–239

Scurfield G, Wardrop AB (1963) The nature of reaction wood. VII. Lignification in reaction wood. Aust J Bot 11:107–116

Sugiyama K, Okuyama T, Yamamoto H, Yoshida M (1993) Generation process of growth stresses in cell walls: relation between longitudinal released strain and chemical composition. Wood Sci Technol 27:257–262

Suzuki K, Itoh T (2001) The changes in cell wall architecture during lignification of bamboo, *Phyllostachys aurea* Carr. Trees 15:137–147

Terashima N (2000) Formation and ultrastructure of lignified plant cell walls. In: Kim YS (ed) New horizons in wood anatomy. Chonnam National University Press, Kwangju, Korea, pp 169–180

Terashima N, Fukushima K (1989) Biogenesis and structure of macromolecular lignin in the cell wall of tree xylem as studied by microautoradiography. In: Lewis NG, Paice MG (eds) Plant cell wall polymers: biogenesis and biodegradation. ACS Symposium Series 399. American Chemical Society, Washington, D.C. pp 160–168

Terashima N, Fukushima K, He LF, Takabe K (1993) Comprehensive model of the lignified plant cell wall. In: Jung HG, Buxton DR, Hatfield RD, Ralph J (eds) Forage cell wall structure and digestibility. American Society of Agronomy, Crop Science Society of America, Soil Science Society of America, Madison, pp 247–270

Wardrop AB (1965) The formation and function of reaction wood. In: Côté WA Jr (ed) Cellular ultrastructure of woody plants. Syracuse University Press, Syracuse, pp 371–390

Wilson BF, Gartner BL (1996) Lean in red alder (*Alnus rubra*). Growth stress, tension wood, and righting response. Can J For Res 26:1951–1956

Yamamoto H (1998) Generation mechanism of growth stresses in wood cell walls: roles of lignin deposition and cellulose microfibril during cell wall maturation. Wood Sci Technol 32:171–182

Yamamoto H, Okuyama T, Yoshida M, Sugiyama K (1991) Generation process of growth stresses in cell walls. III. Growth stress in compression wood. Mokuzai Gakkaishi 37:94–100

Yamamoto H, Okuyama T, Sugiyama K, Yoshida M (1992) Generation process of growth stresses in cell walls. IV. Action of the cellulose microfibril upon the generation of the tensile stresses. Mokuzai Gakkaishi 38:107–113

Yamamoto H, Okuyama T, Yoshida M (1993a) Generation process of growth stresses in cell walls. V. Model of tensile stress generation in gelatinous fibers. Mokuzai Gakkaishi 39:118–125

Yamamoto H, Okuyama T, Yoshida M (1993b) Method of determining the mean microfibril angle of wood over a wide range by the improved Cave's method. Mokuzai Gakkaishi 39:375–381

Yoshida M, Okuyama T (2002) Techniques for measuring growth stress on the xylem surface using strain and dial gauges. Holzforschung (in press)

Yoshida M, Nakamura T, Yamamoto H, Okuyama T (1999) Negative gravitropism and growth stress in GA_3-treated branches of *Prunus spachiana* Kitamura f. *spachiana* cv. *Plenarosea*. J Wood Sci 46:368–372

Yoshida M, Okuda T, Okuyama T (2000a) Tension wood and growth stress induced by artificial inclination in *Liriodendron tulipifera* Linn. and *Prunus spachiana* Kitamura f. *ascendens* Kitamura. Ann For Sci 57:739–746

Yoshida M, Yamamoto H, Okuyama T (2000b) Estimating the equilibrium position by measuring growth stress in weeping branches of *Prunus spachiana* Kitamura f. *spachiana* cv. *Plenarosea*. J Wood Sci 46:59–62

Yoshida M, Ohta H, Okuyama T (2002) Tensile growth stress and lignin distribution in the cell walls of black locust (*Robinia pseudoacacia*). J Wood Sci 48:99–105

Yoshinaga A, Fujita M, Saiki H (1992) Relationships between cell evolution and lignin structural varieties in oak xylem evaluated by microscopic spectrophotometry with separated cell walls. Mokuzai Gakkaishi 38:629–637

Yoshizawa N, Inami A, Miyake S, Ishiguri F, Yokota S (2000) Anatomy and lignin distribution of reaction wood in two *Magnolia* species. Wood Sci Technol 34:183–196